



Recent paradigm shifts in molecular cardiac imaging—Establishing precision cardiology through novel ^{18}F -labeled PET radiotracers[☆]

Rudolf A. Werner^{a,b,c}, Xinyu Chen^{b,c}, Steven P. Rowe^a, Constantin Lapa^b, Mehrbod S. Javadi^a, Takahiro Higuchi^{b,c,d,*}

^a Division of Nuclear Medicine and Molecular Imaging, The Russell H. Morgan Department of Radiology and Radiological Science, Johns Hopkins University School of Medicine, Baltimore, MD, United States

^b Department of Nuclear Medicine, University Hospital Wuerzburg, Wuerzburg, Germany

^c Comprehensive Heart Failure Center, University Hospital Wuerzburg, Wuerzburg, Germany

^d Okayama University Graduate School of Medicine, Dentistry and Pharmaceutical Sciences, Okayama, Japan

ARTICLE INFO

Keywords:

SPECT
PET
Single-photon emission computed tomography
Positron emission tomography
Myocardial perfusion imaging
MPI
Viability
Innervation
Inflammation
Myocardial infarction
Heart failure
 ^{18}F

ABSTRACT

In nuclear cardiology, numerous single-photon emission computed tomography radiotracers have been advocated to reflect various cardiac metabolic and functional conditions, but positron emission tomography (PET) may offer a more thorough evaluation, mainly due to superior characteristics associated with the latter imaging modality. This shift in recent years has been fueled by the introduction of ^{18}F -labeled PET radiotracers. Due to physical and chemical key properties, these imaging agents allow for more flexibility of imaging protocols and a better employment in the clinic. Potentially rendering perfusion, viability, innervation and inflammation, ^{18}F -labeled PET radiotracers may truly pave the way for a global assessment of the current metabolic and functional status of the heart, e.g. after acute myocardial infarction or for progressed heart failure. The present review aims to provide a precise overview of those recently introduced ^{18}F -labeled cardiac imaging agents and how those state-of-the-art, top-tier radiotracers may redefine precision medicine in cardiology.

© 2019 The Author(s). Published by Elsevier Inc.

This is an open access article under the CC BY-NC-ND license. (<http://creativecommons.org/licenses/by-nc-nd/4.0/>)

Introduction

Recent years have witnessed a paradigm shift in cardiac molecular imaging, in particular from single-photon emission computed tomography (SPECT) towards positron emission tomography (PET) for numerous clinical applications [1–4]. However, short-half-life radiotracers in nuclear cardiology limit the more widespread adoption of PET, e.g. by the use of ultra-short half-life imaging agents such as ^{82}Rb , half-life, 76 s) or ^{11}C -labeled radiotracers (half-life,

20 min) [5,6]. Thus, a great deal of progress has been made by the introduction of ^{18}F -labeled imaging probes. Their long half-life of 110 min allow for a.) the use of dispatch systems (for delivery from central cyclotron facilities), b.) the injection of a lower amount of radioactivity (due to a higher positron yield), c.) high spatial resolution (due to a short positron range) and d.) delayed imaging protocols [7]. In addition, PET agents may benefit from the introduction of fluoride, which in turn increases the stability of a radiopharmaceutical (Table 1) [7]. In light of multiple potential pathophysiological conditions that result in heart failure (HF) along with the wide armamentarium of different treatment options, an expert consensus panel recently proposed a “diamond” approach in the treatment of cardiovascular diseases, i.e. personalized assessments instead of a “one-size-fits-all” therapeutic concept [8]. Notably, cardiac PET radiotracers labeled with ^{18}F target a wide array of different cardiac metabolic conditions and functions. Specifically, these include, but are not limited to: (I.) myocardial perfusion, (II.) viability, (III.) innervation, and (IV.) inflammation [3,7,9,10]. The promising physical and chemical properties of ^{18}F -labeled radiotracers may lay the proper groundwork to target those various pathological conditions in the failing heart, which in turn

[☆] Disclosures: This work was supported by the Competence Network of Heart Failure funded by the Integrated Research and Treatment Center (IFB) of the Federal Ministry of Education and Research (BMBF) and German Research Council (DFG grant HI 1789/3-3 and CH 1516/2-1). The authors declare that they have no conflict of interest. This project has received funding from the European Union's Horizon 2020 research and innovation programme under the Marie Skłodowska-Curie grant agreement No. 701983.

* Corresponding author at: Department of Nuclear Medicine/Comprehensive Heart Failure Center, University of Wuerzburg, Oberduerrbacher Strasse 6, 97080 Wuerzburg, Germany.

E-mail addresses: werner_r1@ukw.de (R.A. Werner), thiguchi@me.com (T. Higuchi).

Table 1
Advantages of ^{18}F -radiochemistry. ^{18}F -FDG = 2-deoxy-2- ^{18}F -fluoro-D-glucose.

	Property	Resulting advantage
Physical	Long half-life of 110 min	<ul style="list-style-type: none"> ✓ More flexibility in the study design [31] ✓ Use of dispatch system, which enables delivery from central cyclotron facilities to smaller PET imaging centers (proven to be cost-effective for the most commonly used radiotracer in oncology, ^{18}F-FDG) [7,12] ✓ Allows for physical exercise stress testing outside of the PET device (shorter half-life PET agents allow only for stress imaging under pharmacological stress) [3]
	Short positron range	<ul style="list-style-type: none"> ✓ Enables higher spatio-temporal resolution in tissue [3]
	Lower positron energy	<ul style="list-style-type: none"> ✓ Allows for the injection of less radioactivity [52]
Chemical	Fluoride Introduction	<ul style="list-style-type: none"> ✓ Increases the stability of a radiopharmaceutical against metabolism at sensitive positions [7] ✓ Higher selectivity towards specific targets [7] ✓ Higher flexibility in synthesizing novel PET radiotracers with more complex structures and increased efficacy [7]

may contribute to such a “diamond” approach of tailoring treatment regimens. In addition, such radiotracers could be available at reasonable prices, as the long half-life of ^{18}F permits delivery of unit doses from a regional cyclotron to external PET imaging centers [11]. This strategy has already been proven to be cost-effective for the most commonly used imaging probe in oncology, namely 2-deoxy-2- ^{18}F -fluoro-D-glucose (^{18}F -FDG) [12]. In the present review, we aim to provide a precise overview of such ^{18}F -labeled cardiac radiotracers, which enables identifying the different etiologies in HF. Striving for a global assessment of cardiac functions including perfusion, viability, innervation and inflammation, those imaging agents may establish precision medicine in cardiology and guide the cardiologist in making the appropriate diagnosis early and accurately.

Myocardial perfusion

An integrative assessment of both myocardial perfusion and viability are of utmost importance to draw meaningful conclusions on either scar tissue or hibernating myocardium in patients suffering from myocardial infarction (MI) [13]. Several SPECT myocardial perfusion imaging (MPI) radiotracers have been advocated to allow for a reliable reflection of the current perfusion status of the heart [14], but PET MPI offers 3-dimensional capability along with CT-based attenuation correction, increased spatio-temporal resolution and reliable quantification of absolute myocardial blood flow (MBF) [2,7]. In particular, with ^{18}F -labeled MPI radiotracers, exercise stress testing outside the scanner is feasible, which cannot be implemented in the clinic with other short half-life PET MPI imaging agents [3]. In the last decade, two ^{18}F -labeled radiotracers targeting mitochondria have been further evaluated. These are the lipophilic cation ^{18}F -fluorobenzyltriphenyl-phosphonium (^{18}F -FBnTP) and ^{18}F -flurpiridaz (previously referred as ^{18}F -BMS747158-02), which has also been investigated in human [3]. Higuchi et al. tested ^{18}F -flurpiridaz in a permanent and transient occlusion rat model. After permanent ligation of the left coronary artery (LCA), the defect size remained stable, while after transient ischemia (3 min of LCA occlusion), ^{18}F -flurpiridaz redistributed to the induced defect (i.e. tracer redistribution after reperfusion). Radiotracer reinjection further enhanced the normalization process [15]. The concept of redistribution is based on underperfused but viable myocardium, which retains the radiotracer while it washes out of normal myocardial areas, i.e. initial defects appear to normalize [16]. Thus, in this animal model of coronary occlusion, myocardial viability has been assessed as well. Such an approach could be the subject of future studies, e.g. by radiotracer injection under physical stress with early and delayed imaging protocols, which allows observation of such redistribution over the entire imaging protocol. The same research group has also investigated ^{18}F -FBnTP in a dedicated rat model of short-term occlusion and reperfusion. Notably, distinct characteristics of both ^{18}F -labeled MPI PET radiotracers were observed: While ^{18}F -FBnTP demonstrated reten-

tion stability over time, ^{18}F -flurpiridaz slowly restored the defect area (Fig. 1A) [17]. Altogether, the observed kinetics (redistribution after reperfusion) may allow for the use of ^{18}F -flurpiridaz in a similar way to clinical SPECT protocols (stress/rest ^{201}Tl perfusion protocols) and for the assessment of myocardial viability [15,18]. After laying the proper groundwork in a preclinical setting, ^{18}F -flurpiridaz was subject to clinical trials in human. A phase 1 trial demonstrated clear and homogenous myocardial uptake up to 5 h post-injection (liver clearance after 2 h): those findings are of relevance, as the radiotracer is present in the myocardium to allow for radiopharmaceutical administration at peak treadmill exercise [19]. To assess the performance of ^{18}F -flurpiridaz for MBF assessment, 7 healthy subjects with a low likelihood of myocardial ischemia and 8 coronary artery disease (CAD) patients were enrolled. Lower MBF in diseased vascular segments after adenosine stress was recorded and accompanied by a reduction in myocardial flow reserve (MFR), while subjects with no stress-inducible ischemia demonstrated no such findings [20]. A recent phase II trial underlined the promising properties of ^{18}F -flurpiridaz: In 143 subjects, both stress-rest PET and $^{99\text{m}}\text{Tc}$ sestamibi SPECT were performed. First, the reader's confidence in imaging interpretation was 20% higher for PET. Second, a subcohort was also scheduled for invasive coronary angiography (ICA), serving as the gold standard. In patients with ICA proven CAD, the extent of the reversible defect assessed with PET was larger than with SPECT (Fig. 1B) [21]. A recent phase III trial corroborated the superior diagnostic accuracy of ^{18}F -flurpiridaz relative to SPECT MPI in CAD. Due to improvements in imaging quality, obese subjects seemed to benefit from the use of the ^{18}F -labeled radiotracer [22]. In a second phase III study (AURORA, ClinicalTrials.gov Identifier: NCT03354273), patients will undergo both SPECT and ^{18}F -flurpiridaz PET MPI prior to ICA. In a head-to-head comparison, the diagnostic accuracy of both MPI modalities will be tested to further determine the role of CAD detection with ^{18}F -flurpiridaz [23,24].

Myocardial viability

To date, the most widely used PET radiotracer for evaluating myocardial viability is ^{18}F -FDG. As a marker of glucose utilization, it is taken up into the cardiomyocyte via glucose transporters GLUT1 and 4, followed by a phosphorylation to ^{18}F -FDG-6-phosphate (by hexokinase). Notably, phosphatase, which is needed to convert ^{18}F -FDG-6-phosphate back to its original structure ^{18}F -FDG, is not available in the myocardium [13]. Thus, one may hypothesize that the increase of ^{18}F -FDG-6-phosphate precisely reflects the overall rate of GLUT transport and hexokinase activity. Oral glucose loading or co-infusion of insulin and glucose are routinely employed in the clinic to improve diagnostic accuracy of ^{18}F -FDG PET. Myocardial uptake of ^{18}F -FDG increases due to endogenous release of insulin and succeeding increased glucose utilization along with inhibitory release effects of free fatty acids from adipocytes [13]. As an underlying pathologic rationale,

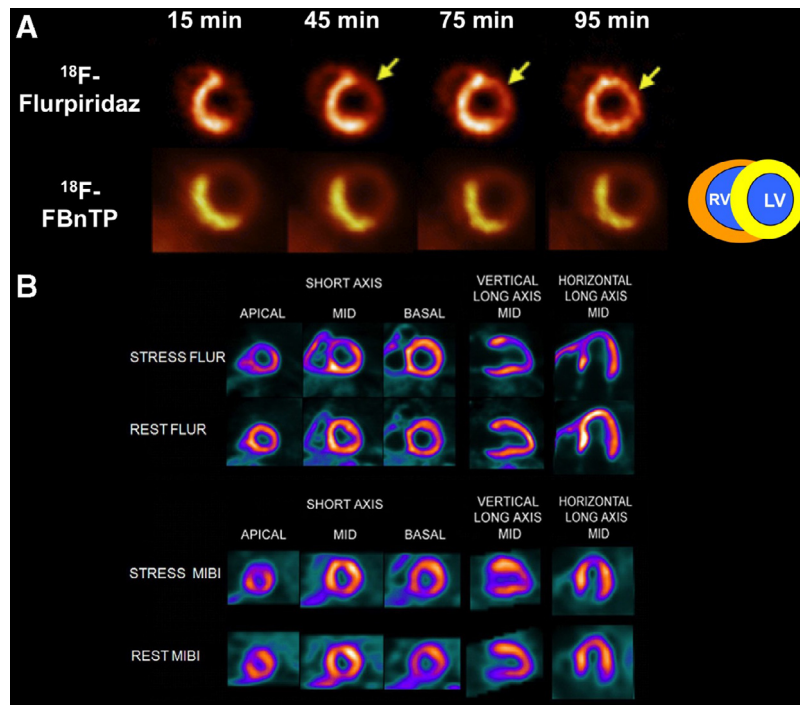


Fig. 1. (A) ^{18}F -labeled myocardial perfusion (MPI) positron emission tomography (PET) radiotracers in a rat model of short-term occlusion and reperfusion. ^{18}F -flurpiridaz and ^{18}F -fluorobenzyltriphenyl-phosphonium (^{18}F -FBnTP) were injected during ischemia. While ^{18}F -flurpiridaz demonstrated slow restoration of uptake, ^{18}F -FBnTP showed lack of washout [3]. This renders ^{18}F -flurpiridaz as a potential imaging agent for myocardial viability (stress/rest protocols similar to thallium 201). Modified from Higuchi et al. [15,17] © by the Society of Nuclear Medicine and Molecular Imaging, Inc. (B) FLUR PET and MIBI SPECT Images From an 82-Year-Old Man. The FLUR PET (top) and MIBI SPECT (bottom) images from an 82-year-old man with shortness of breath and an occluded native proximal left anterior descending (LAD) coronary artery and an occluded left internal mammary graft to the LAD and no other significant native CAD. The FLUR images show a severe reversible perfusion defect throughout the territory of the occluded proximal LAD, whereas the MIBI images show only a moderate perfusion defect in the distal LAD territory (apical slices). FLUR = flurpiridaz F 18; MIBI = Tc-99m sestamibi. Reprinted from the Journal of the American College of Cardiology (JACC), 61(4), Daniel S. Berman, Jamshid Maddahi, B. K. Tamarappoo, Johannes Czernin, Raymond Taillefer, James E. Udelson, C. Michael Gibson, Marybeth Devine, Joel Lazewatsky, Gajanan Bhat, Dana Washburn, Phase II safety and clinical comparison with single-photon emission computed tomography myocardial perfusion imaging for detection of coronary artery disease: flurpiridaz F 18 positron emission tomography, 469-77, Copyright (2013), with permission from Elsevier [21].

ischemic cardiomyopathy can be either associated with development of myocardial scar (i.e. irreversible injury of cardiomyocytes) or hibernating myocardium (i.e. temporary loss of the ability of contraction within an area of viable tissue) [13]. The latter condition can be treated by an invasive revascularization procedure, which underpins the importance of a reliable segregation between irreversible vs. reversible cardiac injury. Thus, ^{18}F -FDG cardiac imaging is routinely applied with MPI (either with SPECT or PET radiotracers), as distinctive patterns of perfusion vs. viability allow identifying potential candidates for catheter-based interventions [13]. These are: (I.) preserved MP and viability, i.e. normal conditions, (II.) reduced MP vs. preserved viability, i.e. mismatch characterized by viable hibernation, (III.) both reduced, i.e. a non-viable match and (IV.) preserved perfusion, but reduced glucose metabolism in the heart, i.e. reversed mismatch pattern (altered regional glucose metabolism) [13]. The second pattern in a dual-tracer assessment reflects hibernating myocardium and is associated with a remarkably better outcome. For instance, vom Dahl et al. showed that discordance of flow and metabolic status have a high predictive value for potential functional recovery after revascularization in areas of varying degrees of reduced left ventricular ejection fraction (LVEF) [25]. The Recovery Following Revascularization-2 (PARR-2) trial further corroborated these findings in a randomized setting; patients diagnosed with ischemic cardiomyopathy and higher degrees of mismatch (>7%) benefited from revascularization (Fig. 2) [26]. Thus, such a dual-tracer assessment may guide the referring cardiologist towards an invasive procedure [13,26]. In addition, the *Institute For Clinical Evaluative Sciences* (ICES, Canada) concluded in an economic analysis that the

use of PET for the assessment of myocardial viability led to a remarkable cost reduction. The use of ^{18}F -FDG PET as a follow-up tool led to a better 5-year survival rate and less cost compared to thallium (^{201}Tl) SPECT [27]. Apart from that, a reversed mismatch pattern (preserved perfusion vs. reduced glucose consumption) has been linked to patients with left bundle branch block, most likely caused by alteration in the metabolic demand of glucose in the septum [28]. Other potential factors include stunning myocardium, e.g. reperfused MI or percutaneous coronary interventions (PCI) followed by coronary vasospasm [29].

Neurohumoral activation

Neurohumoral conditions of the heart are routinely imaged with the SPECT radiotracer ^{123}I -meta-Iodobenzylguanidine (^{123}I -mIBG) [30]. As an underlying rationale on a subcellular level, those neurohumoral radiotracers mimic physiological norepinephrine (NE) turnover in the myocardium and thus reflect precisely the current status of cardiac nerve integrity. Physiological NE is stored in presynaptic vesicles and once a firing impulse has arrived at the nerve terminal, NE is released into the synaptic cleft where it provokes further downstream cascades via adrenoceptors located at the post-synapse [1]. Thereafter, NE is involved in a recycling pathway via the presynaptic NE transporter (NET, uptake-1), and is stored in presynaptic vesicles for the next firing impulse. Radiolabeled NE analogues, also referred to as “false neurotransmitters”, use the identical uptake-1 mechanism and thus, alterations in NE uptake correlate with either decreased radiotracer uptake or increased tracer washout [1]. In

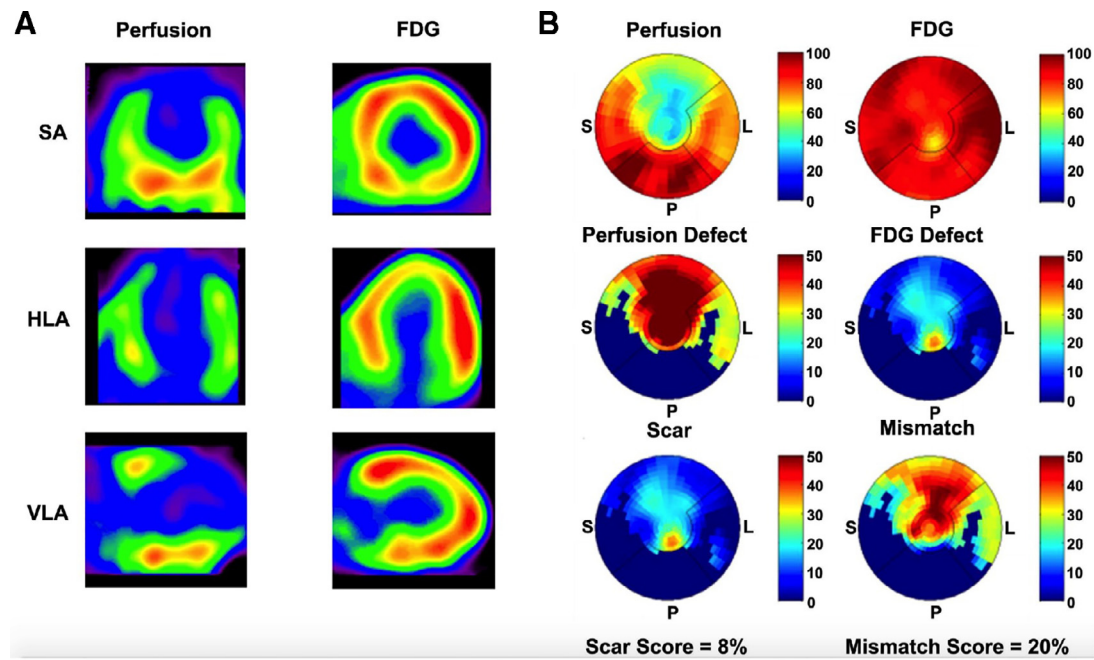


Fig. 2. Examples of Images and Reconstructed Polar Maps. (A) Perfusion (left) and F-18-fluorodeoxyglucose (FDG) (right) imaging in the short-axis (SA), vertical-long-axis (VLA), and horizontal-long-axis (HLA) planes. Reduced perfusion with predominately maintained FDG uptake (mismatch) is noted in the anterior, septal, and lateral walls of the left ventricle (LV). (B) Polar maps (scale is %): top row showing the raw perfusion (left) and raw FDG uptake (right) polar maps; middle row is the normalized perfusion defect and FDG defect; lowest row is the scar score (left) and mismatch score (right). Of the total LV myocardium, 8% was scar, and 20% was mismatch. The patient was referred for revascularization but died within 1 week, awaiting surgery. Reprinted from the Journal of the American College of Cardiology (JACC) Imaging, 2 [9], Gianni D'Egidio, Graham Nichol, Kathryn A. Williams, Ann Guo Meng, Linda Garrard, Robert de Kemp, Terrence D. Ruddy, Jean DaSilva, Dennis Humen, Karen Y. Gulenchyn, Michael Freeman, Normand Racine, Francois Benard, Paul Hendry, Rob S. B. Beanlands, PARR-2 Investigators. Increasing Benefit From Revascularization Is Associated With Increasing Amounts of Myocardial Hibernation: A Substudy of the PARR-2 Trial, 1060 – 1068, Copyright (2009), with permission from Elsevier [26].

a similar vein like for MPI, PET cardiac radiotracers have several key advantages over SPECT, in particular for the assessment of regional areas of denervated myocardium instead of a global reflection of the entire heart, e.g. with ^{123}I -mIBG [31]. Thus, recent years have witnessed a shift from neurohumoral SPECT to PET radiotracers, e.g. with ^{11}C -hydroxyephedrine (^{11}C -HED). However, the short half-life of the latter radiotracer limits its more widespread adoption in the clinic and thus ^{18}F -labeled radiotracers to assess loss of cardiac nervous function are currently at the forefront to monitor cardiac nerve integrity. These are N-[3-Bromo-4-(3-[^{18}F]fluoro-propoxy)-benzyl]guanidine (^{18}F -LMI1195) as well as ^{18}F -Fluoro-Hydroxyphenethylguanidines (^{18}F -fluoro-3-hydroxyphenethylguanidine (^{18}F -4F-MHPG) and its structural isomer 3- ^{18}F -fluoro-4-hydroxyphenethylguanidine (^{18}F -3F-PHPG)) [1]. The most extensively investigated ^{18}F -labeled radiotracer is ^{18}F -LMI1195. First, several *in-vitro* and *in-vivo* tests confirmed the high specificity of this imaging agent towards uptake-1, mainly by performing blocking studies with the potent and selective uptake-1 blocker desipramine (DMI, a tricyclic antidepressant) [31,32]. However, to further corroborate that ^{18}F -LMI1195 closely mimics physiological NE turnover, this radiotracer was also subject to studies investigating whether it is stably stored inside presynaptic vesicles after being taken up via the presynaptic uptake-1. In an *in-vivo* head-to-head comparison using healthy rabbits, the catecholamine analogue radiotracers ^{123}I -mIBG, ^{11}C -HED and ^{18}F -LMI1195 were tested. Distinct radiotracer characteristics were demonstrated: By using a DMI chase protocol (i.e. DMI administered after tracer administration), retention kinetics of the benzylguanidine-based radiotracers ^{123}I -mIBG and ^{18}F -LMI1195 remained stable, while ^{11}C -HED washout increased significantly. Thus, being resistant to such a NET inhibitor chase protocol, it can be concluded that ^{123}I -mIBG and ^{18}F -LMI1195 are stably stored in presynaptic vesicles, while ^{11}C -HED undergoes a cycle of con-

tinuous release and reuptake through uptake-1 mechanism. Altogether, ^{123}I -mIBG and ^{18}F -LMI1195 indeed closely mimic physiological NE, with the latter radiotracer having all the advantages of PET technology (Fig. 3A–C) [31]. After laying the proper groundwork using dedicated animal and cell models, ^{18}F -LMI1195 was tested in humans as well. In a phase I trial, the radiotracer showed stable and uniform myocardial activity up to 5 h post-injection along with rapid blood clearance. Notably, an excellent heart-to-liver ratio was demonstrated, which in turn allows for a precise evaluation of the inferior wall portion as well (Fig. 3D) [33]. In a phase II trial, a head-to-head comparison of ^{18}F -LMI1195 and ^{11}C -HED was performed and a preliminary assessment in 9 participants revealed comparable findings in cardiac nerve integrity. However, ^{18}F -LMI1195 demonstrated superior diagnostic accuracy, in particular for early cardiac imaging [34]. In light of these encouraging results of both phase I/ II trials, a phase III trial is underway to establish the benefits of ^{18}F -LMI1195 in a clinical setting, e.g. for risk stratification among HF, similar to its SPECT counterpart ^{123}I -mIBG [1]. ^{18}F -Fluoro-Hydroxyphenethylguanidines (^{18}F -4F-MHPG and ^{18}F -3F-PHPG) need complex kinetic (Patlak) analyses, but their underlying kinetic properties may allow for the assessment of even the slightest alterations in cardiac nervous function [35]. Notably, these agents have just recently been investigated in human volunteers and a reproducible measurement of cardiac nerve function along with considerable low radiation exposure was reported [36].

Inflammatory activity

In the last decades, several studies have proven the relevance of ^{18}F -FDG for the assessment of inflammation in the myocardium. For instance, it was recently demonstrated that longitudinal ^{18}F -FDG PET imaging has favorable properties to differentiate

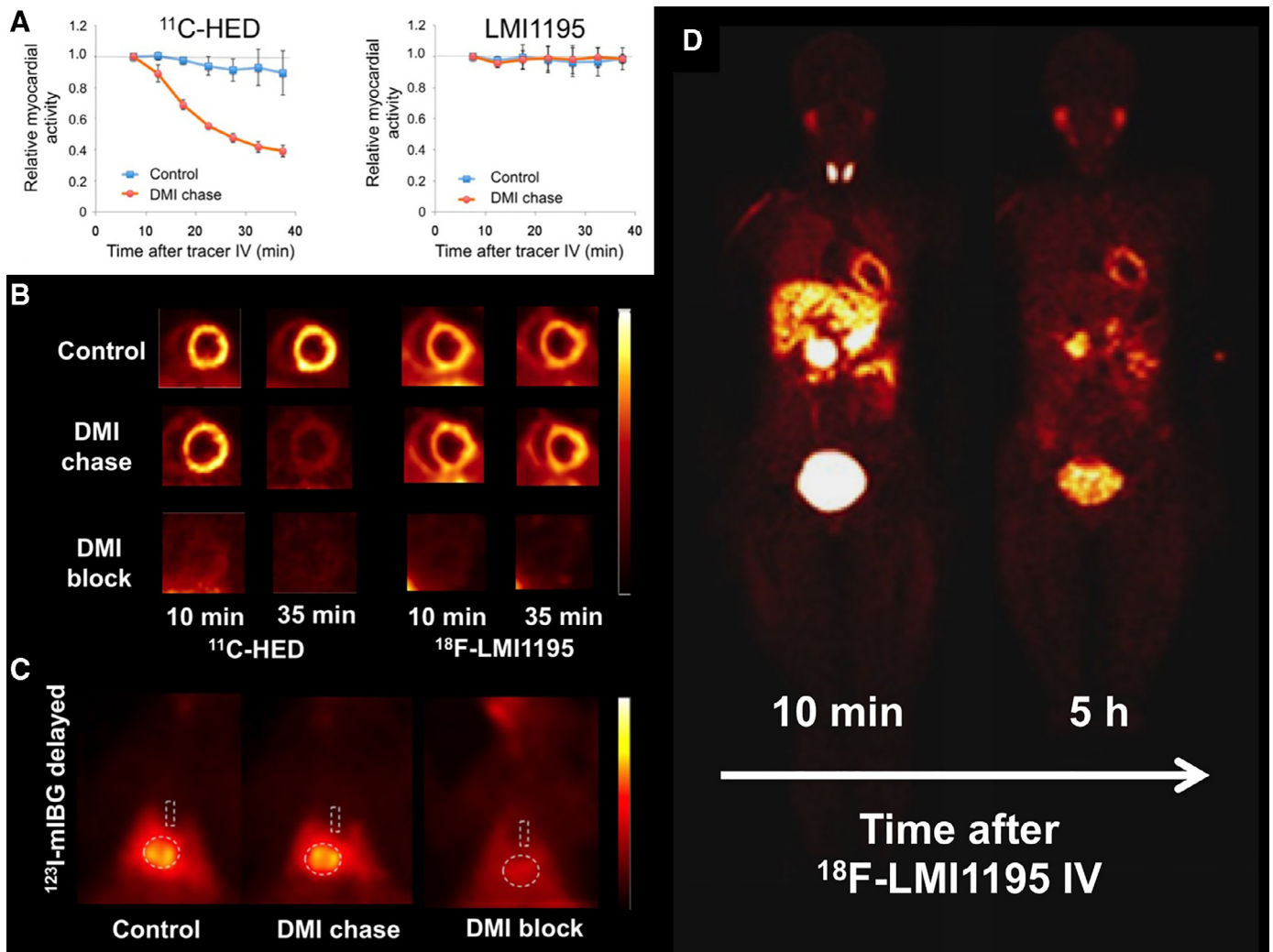


Fig. 3. (A) Averaged time activity curves and (B) representative short-axis images of in-vivo rabbit cardiac PET imaging. Desipramine (DMI) chase (i.e., DMI administered after tracer delivery) enhanced ^{11}C -Hydroxyephedrine (^{11}C -HED) tracer washout, while ^{18}F -N- [3-Bromo-4-(3- [18F]fluoro-propoxy)-benzyl]guanidine (^{18}F -LMI1195) washout remained stable. (C) Results of in-vivo rabbit ^{123}I -metaiodobenzylguanidine (^{123}I -mIBG) planar scintigraphy (SPECT) of the chest. Dotted lines indicate regions of interest in both heart and mediastinum. Similar to ^{18}F -LMI1195, DMI chase did not change cardiac distribution of ^{123}I -mIBG. This indicates stable storage inside the nerve terminal independent of norepinephrine (NE) transporter activity after initial transport. Thus, ^{18}F -LMI1195 indeed closely mimics physiological NE turnover at the sympathetic nerve terminal. Notably, ^{18}F -LMI1195 inherits all advantages of PET technology, along with the key properties of an ^{18}F radionuclide, such as superior imaging quality compared to short-living PET radioisotopes like ^{11}C -HED. Apart from that, all tested tracers (^{18}F -LMI1195, ^{11}C -HED and ^{123}I -MIBG) had a high affinity for neural uptake as demonstrated by the DMI blockade (DMI block, i.e. pretreatment of DMI prior to radiotracer injection, B and C). Modified from Werner et al. [31] © by the Society of Nuclear Medicine and Molecular Imaging, Inc and from Werner et al. [1]. (D) Representative sequences of whole-body ^{18}F -LMI1195 images in healthy volunteers 10 min and 5 h post-injection. A clear delineation of the heart along with low liver and lung uptake can be appreciated, in particular at the late imaging time-point. Modified from Sinusas et al., [33] © by the Society of Nuclear Medicine and Molecular Imaging, Inc. IV = intravenous injection.

between active from postinflammatory reaction. In a dedicated rat autoimmune myocarditis model, myocarditis rats revealed a temporal increase in ^{18}F -FDG uptake (peaked at week 3), which was followed by a rapid decline thereafter. First, a close correlation between macrophage infiltration (assessed by CD68 derived from extracted hearts) and ^{18}F -FDG uptake was shown. Moreover, guided by longitudinal ^{18}F -FDG imaging, an exchange of the adhesive molecules CD44 (acute inflammatory marker) and CD34 (post-inflammation marker) was demonstrated: CD44 positivity was primarily observed at tissue samples obtained at acute phase (i.e. at peak ^{18}F -FDG uptake), while CD34-positive staining areas were predominantly identified in samples harvested at both sub-acute and chronic phases (i.e. at ^{18}F -FDG decrease) [10]. Thus, ^{18}F -FDG may hold the promise to distinguish between acute and post-inflammatory reaction, which in turn allows for PET-guided endomyocardial biopsies in myocarditis or tailored treatment

strategies, e.g. by escalating immunosuppressive therapy at the right time (Fig. 4A–D). The capability of ^{18}F -FDG for a direct interrogation of infiltrating immune cells on a subcellular level has also been proven in a human setting by using PET-guided biopsies in subjects with clinically suspected active myocarditis [37]. In a similar vein, response assessment to prednisolone with ^{18}F -FDG was also performed in a small cohort suffering from Takayasu arteritis [38]. Rischpler et al. investigated 49 patients with ST-segment elevation MI to explore the prognostic value of ^{18}F -FDG PET in combination with magnetic resonance imaging (MRI) in a prospective setting. An ^{18}F -FDG PET/MRI five days after PCI was followed by a succeeding cardiac MRI 6–9 months later. First, the extent of the ^{18}F -FDG signal and circulating leukocytes to peripheral blood (measured by CD14high/ CD16+ monocytes) correlated significantly with the infarction size. Second, the intensity of the ^{18}F -FDG signal was also associated with MRI-derived LV

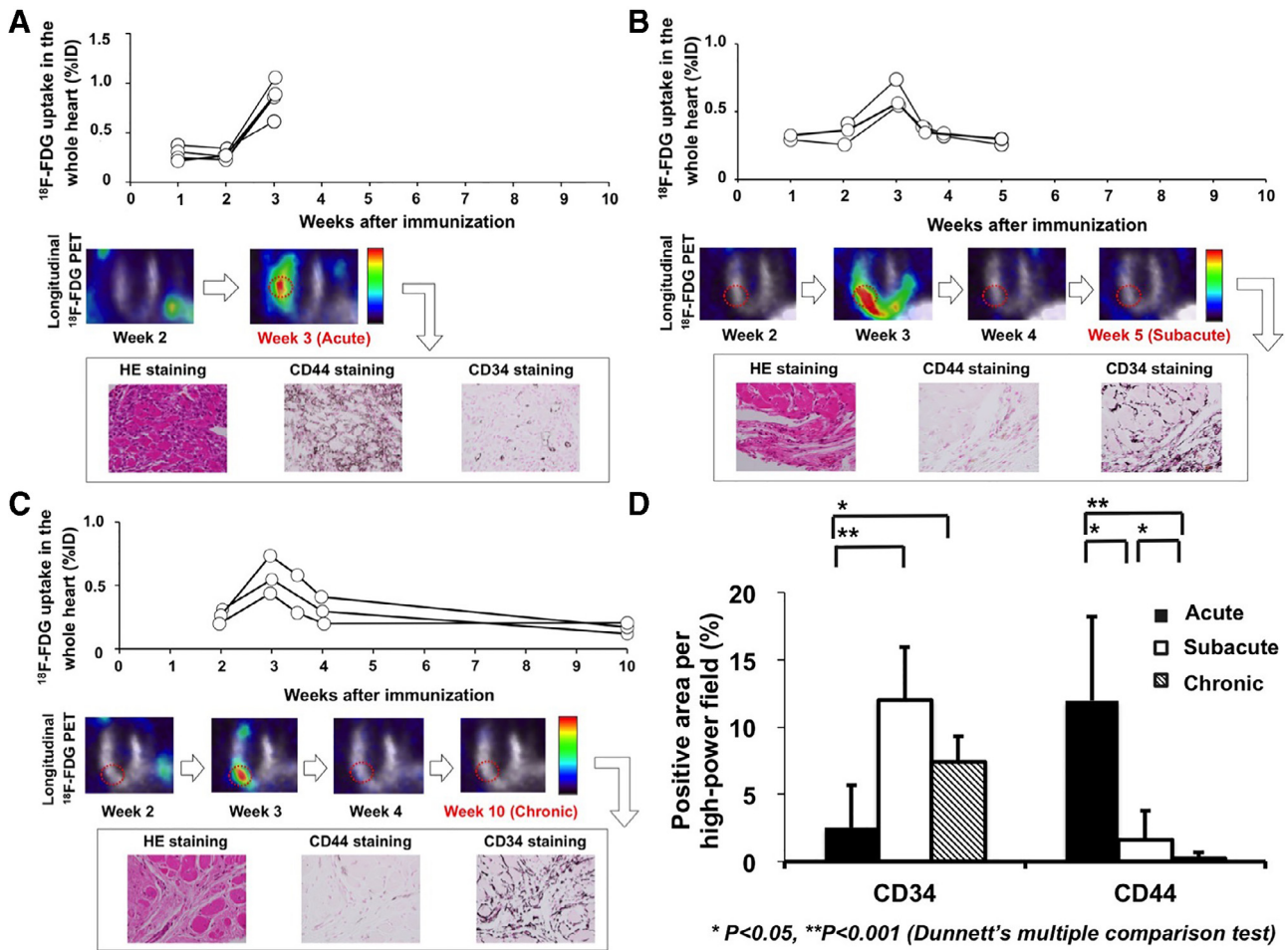


Fig. 4. Exchange of adhesion molecules CD34 and CD44, guided by longitudinal in-vivo ^{18}F -FDG PET imaging in a rat model of autoimmune myocarditis. (A) At acute phase (3 weeks after immunization), a peak ^{18}F -FDG uptake was recorded, with corresponding CD44 positive stained myocardial areas. (B) At subacute phase (5 weeks post-immunization) and (C) chronic phase (10 weeks post-immunization), PET revealed a decline of cardiac tracer uptake: An increase in CD34 positivity was noted, whereas a further decrease of CD44 positively stained cells could be identified. (D) Quantitative analysis of adhesion markers at different phases revealed a low CD34 and – conversely – an increased CD44 positivity (in%) at acute phase. At both subacute and chronic phases, opposite findings with CD34 positively stained areas and a further decrease in CD44 positivity were recorded. Modified from Werner et al. [10]. This paper has been published in the European Heart Journal Cardiovascular Imaging. The version of record "Werner RA, Wakabayashi H, Bauer J, Schütz C, Zechmeister C, Hayakawa N, Javadi MS, Lapa C, Jahns R, Ergün V, Higurashi T; Longitudinal ^{18}F -FDG PET Imaging in a Rat Model of Autoimmune Myocarditis" is available online at <https://doi.org/10.1093/ehjci/jej119>.

global and functional outcome measures, which was not dependent on infarct size or monocytes: In a multivariable analysis, only the ^{18}F -FDG-based mean standardized uptake value served as an independent marker for LV outcome. Integrating these available data, this novel imaging-guided concept may open avenues to visualize immune cell migration to the myocardium and identify patients most at risk for developing HF after MI. Most importantly, ^{18}F -FDG PET may even guide immunomodulatory therapies once those have been added to the armamentarium of treatment options in HF [39]. Further studies, which allow segregation between different myocardial inflammatory diseases based on ^{18}F -FDG PET, are warranted, e.g. by investigating uptake patterns/signaling, imaging timepoints or radiotracer dosing/kinetics among patients suffering from different cardiac diseases (such as MI vs. myocarditis). However, it has been hypothesized that other more leukocyte-specific radiotracers than ^{18}F -FDG may allow for a more thorough evaluation of inflammation in the myocardium [10]. For instance, Thackeray et al. have recently tested the novel ^{18}F -labeled PET imaging agent ^{18}F -flutriclamide (^{18}F -GE180). This radiotracer targets the mitochondrial translocator protein (TSPO), which is predominantly overexpressed on activated macrophages [40]. In an

elegant way, the authors assessed the impact of MI on cardiac and brain inflammation hypothesizing a potential systemic interaction. In an acute MI model in mice, the early TSPO signal predicted subsequent LV remodeling at week 8, paralleled by an elevated TSPO signal in the brain at week 1. Notably, progressive HF after MI caused a second wave of neuroinflammation and treatment with angiotensin-converting enzyme inhibitors led to marked reduction of acute inflammatory activity both in the heart and the brain (accompanied by improvement in cardiac function). Those findings were further corroborated in humans: compared to controls, an elevation of TSPO was noted in the infarct area that was paralleled by neuroinflammation. Thus, defining a potential reciprocable involvement of the heart-brain axis, the authors concluded that the brain seems to be susceptible to acute MI, which in turn may enable more embracing treatment concepts for both the heart and the brain [40]. Kashiyama et al. also reported on the use of another ^{18}F -labeled radioligand for TSPO imaging, namely N,N-diethyl-2-[4-(2-fluoroethoxy) phenyl]-5,7-dimethylpyrazolo [1,5-a]pyrimidine-3-acetamide (DPA-714). It was proven that ^{18}F -DPA-714 visualizes macrophage-mediated immune rejection of transplanted iPSC-derived cardiomyocytes of allogeneic origin [41].

Table 2

Overview of different ^{18}F -labeled radiotracers targeting various cardiac subcellular mechanism. ^{18}F -FBnTP = ^{18}F -fluorobenzyltriphenyl-phosphonium, SPECT = single photon emission computed tomography, PET = positron emission tomography, FDA = U.S. Food and Drug Administration, ^{18}F -FDG = 2-deoxy-2- ^{18}F -fluoro-D-glucose, GLUT = glucose transporter, PARR-2 = Recovery Following Revascularization-2, ^{18}F -LMI1195 = N-[3-Bromo-4-(3- [18F]fluoro-propoxy)-benzyl]guanidine, NET = norepinephrine transporter, ^{11}C -HED = ^{11}C -hydroxyephedrine, ^{18}F -4F-MHPG = ^{18}F -fluoro-3-hydroxyphenethylguanidine, ^{18}F -3F-PHPG = 3- ^{18}F -fluoro-4-hydroxyphenethylguanidine, MI = myocardial infarction, HF = heart failure, ^{18}F -GE180 = ^{18}F -flutriclamide, ^{18}F -DPA-714 = N,N-diethyl-2-[4-(2-fluoroethoxy) phenyl]-5,7-dimethylpyrazolo [1,5-a]pyrimidine-3-acetamide.

Targeting	Radio-tracer	Subcellular mechanism	Key characteristics	Clinical use and current trial status
Myocardial perfusion	^{18}F -flurpiridaz	Mitochondrial complex I	<ul style="list-style-type: none"> ✓ Demonstrated tracer redistribution after reperfusion, i.e. myocardial viability can be assessed [15] ✓ May allow for the use of ^{18}F-flurpiridaz in a similar way to clinical SPECT protocols (stress/rest ^{201}Tl perfusion protocols) [15] ✓ Phase I/ II trials: Extent of the reversible defect assessed with PET was larger than with SPECT and higher reader's confidence in interpretation with ^{18}F-flurpiridaz was noted [19,21] 	<ul style="list-style-type: none"> ✓ No clinical routine use, but a Special Protocol Assessment has been granted by the FDA [53] ✓ Currently being investigated in a phase III study
	^{18}F -FBnTP	Mitochondria localization via membrane potential	<ul style="list-style-type: none"> ✓ Primarily used in a preclinical setting [17] 	<ul style="list-style-type: none"> ✓ No clinical routine use, no FDA approval
Myocardial viability	^{18}F -FDG	GLUT transport and hexokinase activity	<ul style="list-style-type: none"> ✓ Routinely employed in the clinic to assess potential mismatch between perfusion and viability (detection of potential hibernating myocardium) [13] ✓ PARR-2 trial: patients diagnosed with ischemic cardiomyopathy and higher degrees of perfusion/viability mismatch (>7%) had a benefit from revascularization [26] ✓ Remarkable cost reduction compared to ^{201}Tl SPECT for follow-up assessments of myocardial viability [27] 	<ul style="list-style-type: none"> ✓ FDA approved, in clinical routine use
Neuro-humoral activation	^{18}F -LMI1195	NET (uptake-1) at the presynaptic nerve terminal	<ul style="list-style-type: none"> ✓ Demonstrated excellent key properties closely mimicking physiological norepinephrine turnover [31,32] ✓ Phase I trial showed stable myocardial activity up to 5 h post-injection and a radiation dose comparable to other PET radiotracers [33] ✓ Phase II trial: head-to-head comparison of ^{18}F-LMI1195 and ^{11}C-HED, with ^{18}F-LMI1195 having superior diagnostic accuracy, in particular for early cardiac imaging [34] 	<ul style="list-style-type: none"> ✓ No clinical routine use, no FDA approval ✓ Phase III trial is underway
	^{18}F -4F-MHPG, ^{18}F -3F-PHPG		<ul style="list-style-type: none"> ✓ Need Patlak analyses and their kinetic properties may allow for the assessment of even the slightest alterations in cardiac nervous function [35] ✓ First in-human evaluations showed excellent imaging quality along with reproducible measurements of cardiac nerve function and a slow NET rate [36] 	<ul style="list-style-type: none"> ✓ No clinical routine use, no FDA approval
Inflammation	^{18}F -FDG	Macrophages, cell migration	<ul style="list-style-type: none"> ✓ Visualized immune cell migration to the myocardium post-MI and may identify patients at risk for progressed HF [39] ✓ Differentiated between acute and post-inflammatory reaction in myocarditis [10] ✓ Monitored immuno-modulatory treatment response in patients suffering from cardiac inflammation [38] 	<ul style="list-style-type: none"> ✓ FDA approved, in clinical routine use
	^{18}F -GE180	Mitochondrial translocator protein	<ul style="list-style-type: none"> ✓ Revealed systemic interaction between heart and brain after MI [40] 	<ul style="list-style-type: none"> ✓ No clinical routine use, no FDA approval
	^{18}F -DPA-714		<ul style="list-style-type: none"> ✓ Visualized macrophages-mediated immune rejection of transplanted iPSC-derived cardiomyocytes [41] 	<ul style="list-style-type: none"> ✓ No clinical routine use, no FDA approval

Table 2 summarizes the herein reviewed ^{18}F -labeled imaging agents for myocardial perfusion, viability, innervation and inflammation.

Future perspectives

Redefining fractional flow reserve for coronary revascularization

In two recent randomized trials (Fractional Flow Reserve versus Angiography for Multivessel Evaluation, FAME and FAME-2), a fractional flow reserve (FFR) cut-off value of 0.8 confirmed that the use of FFR can be used to guide the referring cardiologist towards coronary revascularization [42,43]. Notably, this threshold was originally introduced by noninvasive stress testing, e.g. by ^{201}Tl SPECT [44]. Consequently, FFR has also been recently implemented in current guidelines for patients with ischemic heart disease and

thus such quantitative metrics assessed by MPI SPECT and PET hold the promise of contributing to personalized medicine in cardiology [45,46]. Nonetheless, FFR can also lead to false-positive discoveries in the presence of microvascular dysfunction or disease [46,47]. Thus, given the superior imaging characteristics of ^{18}F -labeled PET MPI radiotracers compared to SPECT or other PET MPI competitors, it is possible that these novel radiotracers may redefine current FFR thresholds.

Impact on clinical decision making and cost-effectiveness

In a prospective, multicenter setting, Udelson et al. have shown that the use of SPECT agents reduces unnecessary hospitalizations among patients without acute ischemia by 10% compared to those subjects evaluated with standard care [48]. Siegrist et al. have attempted the cost savings on cardiac treatment procedures

using the short half-life PET MPI radiotracer ^{13}N -ammonia: In the vast majority of the patients having a high prevalence of known CAD, treatment strategies were altered based on PET imaging findings. Notably, a cost-effectiveness analysis also showed that PET MPI led to a cost reduction of >200 € per patient [49]. In light of the superior imaging properties of ^{18}F -labeled MPI radiotracers compared to other common SPECT or PET MPI imaging agents, agents like ^{18}F -flurpiridaz may have an even more significant impact on clinical decision making. Thus, future studies should determine if these ^{18}F -labeled radiotracers affect the management in CAD patients, if such altered treatment strategies will be implemented by the referring clinicians or if hospital (re)admissions can be avoided.

Triple tracer approaches for a global assessment of cardiac function

The concept of myocardial viability assessment in nuclear cardiology is closely linked to myocardial perfusion [13]. Different patterns of glucose metabolism, mainly derived by ^{18}F -FDG, along with perfusion status guide the referring cardiologists towards revascularization, e.g. for hibernating myocardium [13]. However, it has been recently demonstrated that the area of denervation post-MI exceeded the region defined by MPI: In a transient ischemia rat model (LCA occlusion followed by reperfusion), the extent of denervated myocardium (measured by ^{11}C -HED) was larger compared to the perfusion defect area assessed with ^{201}Tl [50]. Integrating these information, a triple ^{18}F -labeled radiotracer approach for rendering the viability/perfusion/cardiac nerve status may truly mirror a global assessment of current conditions in the failing heart. Apart from that, those radiotracers for measuring cardiac nerve integrity can also be applied to a large variety of other diseases, e.g. in diabetes or in patients at risk for cardiac arrhythmic events [51].

Conclusions

Several SPECT radiotracers have been advocated to reflect various cardiac conditions, but PET may offer a more thorough evaluation of the myocardium, mainly due to the superior imaging properties associated with the latter imaging modality. This shift in recent years has been fueled by the introduction of ^{18}F -labeled PET cardiac radiotracers. Given their multiple physical and chemical key advantages over other PET probes, those imaging agents allow for more flexibility in the study design and a better employment in the clinic. Potentially rendering the perfusion, viability, innervation and inflammation of the myocardium, ^{18}F -labeled PET radiotracers truly pave the way for a global assessment of the current status of the heart, which in turn may be helpful to initiate the appropriate treatment at the right time. Thus, beyond current assessments of perfusion/viability, future efforts may turn towards triple-tracer approaches using those long-living radiotracers, e.g. by performing an additional ^{18}F cardiac nerve PET scan. Moreover, cost-effective analysis on ^{18}F -FDG PET for the assessment of myocardial viability have already proven a significant impact on cost savings in cardiology and thus, similar studies should be performed to determine if implementation of other ^{18}F -labeled agents, e.g. for MPI, may also lead to substantial savings.

References

- Werner RA, Chen X, Hirano M, Rowe SP, Lapa C, Javadi MS, et al. SPECT vs. PET in cardiac innervation imaging: clash of the titans. *Clin Transl Imaging* 2018;6(4):293–303.
- Rowe SP, Gorin MA, Pomper MG. Imaging of prostate-specific membrane antigen using [(18)F]DCFPyL. *PET Clin* 2017;12(3):289–96.
- Rischpler C, Park MJ, Fung GS, Javadi M, Tsui BM, Higuchi T. Advances in PET myocardial perfusion imaging: F-18 labeled tracers. *Ann Nucl Med*. 2012;26(1):1–6.
- Werner RA, Bluemel C, Allen-Auerbach MS, Higuchi T, Herrmann K. ^{68}Ga and ^{90}Tl tracers: "theranostic twins" for diagnosis and treatment of NETs. *Ann Nucl Med* 2015;29(1):1–7.
- Maddahi J, Packard RR. Cardiac PET perfusion tracers: current status and future directions. *Semin Nucl Med* 2014;44(5):333–43.
- Dilsizian V, Bacharach SL, Beanlands RS, Bergmann SR, Delbeke D, Dorbala S, et al. ASNC imaging guidelines/SNMMI procedure standard for positron emission tomography (PET) nuclear cardiology procedures. *J Nucl Cardiol* 2016;23(5):1187–226.
- Kobayashi R, Chen X, Werner RA, Lapa C, Javadi MS, Higuchi T. New horizons in cardiac innervation imaging: introduction of novel (18)F-labeled PET tracers. *Eur J Nucl Med Mol Imaging* 2017;44(13):2302–9.
- Ferrari R, Camici PG, Crea F, Danchin N, Fox K, Maggioni AP, et al. Expert consensus document: a 'diamond' approach to personalized treatment of angina. *Nat Rev Cardiol* 2018;15(2):120–32.
- Gewirtz H, Dilsizian V. Myocardial viability: survival mechanisms and molecular imaging targets in acute and chronic ischemia. *Circ Res* 2017;120(7):1197–212.
- Werner RA, Wakabayashi H, Bauer J, Schutz C, Zechmeister C, Hayakawa N, et al. Longitudinal ^{18}F -FDG PET imaging in a rat model of autoimmune myocarditis. *Eur Heart J Cardiovasc Imaging* 2018.
- Brunken RC. Promising new ^{18}F -labeled tracers for PET myocardial perfusion imaging. *J Nucl Med* 2015;56(10):1478–9.
- Ducharme J, Goertzen AL, Patterson J, Demeter S. Practical aspects of ^{18}F -FDG PET when receiving ^{18}F -FDG from a distant supplier. *J Nucl Med Technol* 2009;37(3):164–9.
- Ghosh N, Rimoldi OE, Beanlands RS, Camici PG. Assessment of myocardial ischaemia and viability: role of positron emission tomography. *Eur Heart J* 2010;31(24):2984–95.
- Betancur JA, Hu LH, Commandeur F, Sharir T, Einstein AJ, Fish MB, et al. Deep learning analysis of upright-supine high-efficiency SPECT myocardial perfusion imaging for prediction of obstructive coronary artery disease: a multicenter study. *J Nucl Med*. 2018.
- Higuchi T, Nekolla SG, Huisman MM, Reder S, Poethko T, Yu M, et al. A new ^{18}F -labeled myocardial PET tracer: myocardial uptake after permanent and transient coronary occlusion in rats. *J Nucl Med* 2008;49(10):1715–22.
- Pagnanelli RA, Basso DA. Myocardial perfusion imaging with ^{201}Tl . *J Nucl Med Technol* 2010;38(1):1–3.
- Higuchi T, Fukushima K, Rischpler C, Isoda T, Javadi MS, Ravert H, et al. Stable delineation of the ischemic area by the PET perfusion tracer ^{18}F -fluorobenzyl triphenyl phosphonium after transient coronary occlusion. *J Nucl Med* 2011;52(6):965–9.
- Rischpler C, Higuchi T, Fukushima K, Javadi MS, Merrill J, Nekolla SG, et al. Transient ischemic dilation ratio in ^{82}Rb PET myocardial perfusion imaging: normal values and significance as a diagnostic and prognostic marker. *J Nucl Med* 2012;53(5):723–30.
- Maddahi J, Czernin J, Lazewatsky J, Huang SC, Dahlbom M, Schelbert H, et al. Phase I, first-in-human study of BMS747158, a novel ^{18}F -labeled tracer for myocardial perfusion PET: dosimetry, biodistribution, safety, and imaging characteristics after a single injection at rest. *J Nucl Med* 2011;52(9):1490–1498.
- Packard RR, Huang SC, Dahlbom M, Czernin J, Maddahi J. Absolute quantitation of myocardial blood flow in human subjects with or without myocardial ischemia using dynamic flurpiridaz F 18 PET. *J Nucl Med* 2014;55(9):1438–44.
- Berman DS, Maddahi J, Tamarappoo BK, Czernin J, Taillefer R, Udelson JE, et al. Phase II safety and clinical comparison with single-photon emission computed tomography myocardial perfusion imaging for detection of coronary artery disease: flurpiridaz F 18 positron emission tomography. *J Am Coll Cardiol* 2013;61(4):469–77.
- Bateman TM, Maddahi J, Udelson J, Beanlands R, Knuuti J, Heller G, et al. Improved assessment of CAD in obese subjects with flurpiridaz F18 PET myocardial perfusion imaging: a subset analysis of the flurpiridaz F18 301 phase 3 study. *JACC* 2016;67(13 Suppl).
- <https://www.medicaldevice-network.com/news/ge-healthcare-initiates-new-phase-iii-trial-flurpiridaz-detect-cad/>, last downloaded August 4, 2018.
- <https://clinicaltrials.gov/ct2/show/study/NCT03354273> – contacts. An International Study to Evaluate Diagnostic Efficacy of Flurpiridaz (^{18}F) Injection PET MPI in the Detection of Coronary Artery Disease (CAD) last downloaded August 5, 2018.
- vom Dahl J, Eitzman DT, al-Aouar ZR, Kanter HL, Hicks RJ, Deeb GM, et al. Relation of regional function, perfusion, and metabolism in patients with advanced coronary artery disease undergoing surgical revascularization. *Circulation* 1994;90(5):2356–66.
- D'Egidio G, Nichol G, Williams KA, Guo A, Garrard L, deKemp R, et al. Increasing benefit from revascularization is associated with increasing amounts of myocardial hibernation: a substudy of the PARR-2 trial. *JACC Cardiovasc Imaging* 2009;2(9):1060–8.
- Health Quality O. Positron emission tomography for the assessment of myocardial viability: an evidence-based analysis. *Ont Health Technol Assess Ser* 2005;5(16):1–167.
- Thompson K, Saab G, Birnie D, Chow BJ, Ukkonen H, Ananthasubramanian K, et al. Is septal glucose metabolism altered in patients with left bundle branch block and ischemic cardiomyopathy? *J Nucl Med* 2006;47(11):1763–8.
- Pomblum VJ, Korbmacher B, Cleveland S, Sunderdiek U, Klocke RC, Schipke JD. Cardiac staging in the clinic: the full picture. *Interact Cardiovasc Thorac Surg* 2010;10(1):86–91.

- [30] Nakajima K, Nakata T. Cardiac 123I-MIBG imaging for clinical decision making: 22-year experience in Japan. *J Nucl Med* 2015;56(Suppl 4):115–19S.
- [31] Werner RA, Rischpler C, Onthank D, Lapa C, Robinson S, Samnick S, et al. Retention kinetics of the 18F-labeled sympathetic nerve PET tracer LMI1195: comparison with 11C-hydroxyephedrine and 123I-MIBG. *J Nucl Med* 2015;56(9):1429–33.
- [32] Chen X, Werner RA, Lapa C, Nose N, Hirano M, Javadi MS, et al. Subcellular storage and release mode of the novel (18)F-labeled sympathetic nerve PET tracer LMI1195. *EJNMMI Res* 2018;8(1):12.
- [33] Sinusas AJ, Lazewatsky J, Brunetti J, Heller G, Srivastava A, Liu YH, et al. Biodistribution and radiation dosimetry of LMI1195: first-in-human study of a novel 18F-labeled tracer for imaging myocardial innervation. *J Nucl Med* 2014;55(9):1445–51.
- [34] Zelt J, Ranaud J, Mielniczuk L, Garrard L, Walter O, Guo A, et al. 1312M-07 - fluorine-18 LMI1195 positron emission tomography provides accurate measure of cardiac sympathetic innervation compared to carbon-11 hydroxyephedrine. Abstract of the 67th Annual Scientific Session & Expo. American College of Cardiology; 2016.
- [35] Raffel D, Jung YW, Murthy V, Gu G, Rothley J, Koeppel R, et al. First-in-human studies of 18F-hydroxyphenethylguanidines: PET radiotracers for quantifying cardiac sympathetic nerve density. *J Nucl Med* 2016;57(suppl 2):232.
- [36] Raffel DM, Jung YW, Koeppel RA, Jang KS, Gu G, Scott PJH, et al. First-in-human studies of [(18)F] fluorohydroxyphenethylguanidines. *Circ Cardiovasc Imaging* 2018;11(12):e007965.
- [37] Ozawa K, Funabashi N, Daimon M, Takaoka H, Takano H, Uehara M, et al. Determination of optimum periods between onset of suspected acute myocarditis and (1)(8)F-fluorodeoxyglucose positron emission tomography in the diagnosis of inflammatory left ventricular myocardium. *Int J Cardiol* 2013;169(3):196–200.
- [38] Kobayashi Y, Ishii K, Oda K, Nariai T, Tanaka Y, Ishiwata K, et al. Aortic wall inflammation due to Takayasu arteritis imaged with 18F-FDG PET coregistered with enhanced CT. *J Nucl Med* 2005;46(6):917–22.
- [39] Rischpler C, Dirschinger RJ, Nekolla SG, Kossmann H, Nicolosi S, Hanus F, et al. Prospective evaluation of 18F-fluorodeoxyglucose uptake in postischemic myocardium by simultaneous positron emission tomography/magnetic resonance imaging as a prognostic marker of functional outcome. *Circ Cardiovasc Imaging* 2016;9(4):e004316.
- [40] Thackeray JT, Hupe HC, Wang Y, Bankstahl JP, Berding G, Ross TL, et al. Myocardial inflammation predicts remodeling and neuroinflammation after myocardial infarction. *J Am Coll Cardiol* 2018;71(3):263–75.
- [41] Kashiwama N, Miyagawa S, Fukushima S, Kawamura T, Kawamura A, Yoshida S, et al. Development of PET imaging to visualize activated macrophages accumulated in the transplanted iPSC-derived cardiac myocytes of allogeneic origin for detecting the immune rejection of allogeneic cell transplants in mice. *PLoS One* 2016;11(12):e0165748.
- [42] Tonino PA, De Bruyne B, Pijls NH, Siebert U, Ikeno F, van' t Veer M, et al. Fractional flow reserve versus angiography for guiding percutaneous coronary intervention. *N Engl J Med* 2009;360(3):213–24.
- [43] De Bruyne B, Pijls NH, Kalesan B, Barbato E, Tonino PA, Piroth Z, et al. Fractional flow reserve-guided PCI versus medical therapy in stable coronary disease. *N Engl J Med* 2012;367(11):991–1001.
- [44] Pijls NH, De Bruyne B, Peels K, Van Der Voort PH, Bonnier HJ, Bartunek JKJ, et al. Measurement of fractional flow reserve to assess the functional severity of coronary-artery stenoses. *N Engl J Med* 1996;334(26):1703–8.
- [45] Windecker S, Kolh P, Alfonso F, Collet JP, Cremer J, et al., Authors/Task Force on myocardial revascularization of the European Society of Cardiology (ESC) and the European Association for Cardio-Thoracic Surgery (EACTS) developed with the special contribution of the European Association of Percutaneous Cardiovascular Interventions (EAPCI). *Eur Heart J* 2014;35(37):2541–619.
- [46] Murthy VL, Bateman TM, Beanlands RS, Berman DS, Borges-Neto S, Chareonthaitawee P, et al. Clinical quantification of myocardial blood flow using PET: joint position paper of the SNMMI cardiovascular council and the ASNC. *J Nucl Cardiol* 2018;25(1):269–97.
- [47] De Bruyne B, Oldroyd KG, Pijls NHJ. Microvascular (Dys)function and clinical outcome in stable coronary disease. *J Am Coll Cardiol* 2016;67(10):1170–2.
- [48] Udelson JE, Beshansky JR, Ballin DS, Feldman JA, Griffith JL, Handler J, et al. Myocardial perfusion imaging for evaluation and triage of patients with suspected acute cardiac ischemia: a randomized controlled trial. *JAMA* 2002;288(21):2693–700.
- [49] Siegrist PT, Husmann L, Knabenhans M, Gaemperli O, Valenta I, Hoefflinghaus T, et al. (13)N-ammonia myocardial perfusion imaging with a PET/CT scanner: impact on clinical decision making and cost-effectiveness. *Eur J Nucl Med Mol Imaging* 2008;35(5):889–95.
- [50] Werner RA, Maya Y, Rischpler C, Javadi MS, Fukushima K, Lapa C, et al. Sympathetic nerve damage and restoration after ischemia-reperfusion injury as assessed by (11)C-hydroxyephedrine. *Eur J Nucl Med Mol Imaging* 2016;43(2):312–18.
- [51] Bengel FM. Imaging of myocardial catecholamine uptake. *Circ Cardiovasc Imaging* 2018;11(12):e008534.
- [52] Werner RA, Wakabayashi H, Chen X, Hirano M, Shinaji T, Lapa C, et al. Functional renal imaging with 2-deoxy-2-(18)F-fluorosorbitol PET in rat models of renal disorders. *J Nucl Med* 2018;59(5):828–32.
- [53] <http://www.lantheus.com/pipeline/flurpiridaz-f-18/> last downloaded February 13, 2019.